Carbohydrate Polymers 89 (2012) 759–767

Contents lists available at SciVerse ScienceDirect

Carbohydrate Polymers

journal homepage: www.elsevier.com/locate/carbpol

Adhesion and micromechanical deformation processes in PLA/$CaSO_4$ composites

Balázs Imre[a,b], Gergely Keledi[a,b], Károly Renner[a,b], János Móczó[a,b], Marius Murariu[c], Philippe Dubois[c], Béla Pukánszky[a,b,*]

[a] Laboratory of Plastics and Rubber Technology, Department of Physical Chemistry and Materials Science, Budapest University of Technology and Economics, H-1521 Budapest, P.O. Box 91, Hungary
[b] Institute of Materials and Environmental Chemistry, Chemical Research Center, Hungarian Academy of Sciences, H-1525 Budapest, P.O. Box 17, Hungary
[c] Laboratory of Polymeric and Composite Materials, Center of Innovation and Research in Materials and Polymers (CIRMAP), Materia Nova Research Center, University of Mons, Place du Parc 20, 7000 Mons, Belgium

ARTICLE INFO

Article history:
Received 23 December 2011
Received in revised form 30 March 2012
Accepted 3 April 2012
Available online 10 April 2012

Keywords:
PLA/$CaSO_4$ bio-composites
Interfacial adhesion
Debonding
Surface modification

ABSTRACT

PLA/$CaSO_4$ composites were prepared from uncoated and stearic acid coated filler particles in a wide composition range. The strength of interfacial adhesion was estimated quantitatively with three independent methods. Structure was characterized by DSC, XRD and SEM measurements, while mechanical properties by tensile and instrumented impact tests. The results proved that adhesion is twice as strong in composites prepared with the uncoated particles than in those containing the coated filler. Coating changes also local deformation processes around the particles. Although debonding is the dominating micromechanical deformation process in all composites, local plastic deformation is larger around coated particles. The extent of this deformation depends very much also on the local distribution of particles. The final properties and performance of the composites depend unambiguously on the micromechanical deformation processes occurring during loading, on debonding and the subsequent plastic deformation. Stearic acid used for the coating of the filler seems to dissolve in the polymer and locally change its properties.

1. Introduction

The quest for replacing fossil fuel based polymers with materials from renewable resources has started some time ago and has been going on continuously in the last one or two decades (Belgacem & Gandini, 2008; Evans, 2011; Gandini, 2008; Lindblad, Liu, Albertsson, Ranucci, & Karlsson, 2002; Mohanty, Misra, & Drzal, 2002; Williams & Hillmyer, 2008). One of the candidates to replace hydrocarbon polymers is poly(lactic acid) (PLA). Considerable effort is done to use this polymer in various applications as well as to modify it by copolymerization (Auras, Harte, & Selke, 2004; Hirata & Kimura, 2008; Ho, Wang, Lin, & Lee, 2008; Li et al., 2008; Mert, Doganci, Erbil, & Dernir, 2008; Nagahama, Nishimura, Ohya, & Ouchi, 2007; Södergard & Stolt, 2002), blending (Gu, Zhang, Ren, & Zhan, 2008; Rohman, Laupretre, Boileau, Guerin, & Grande, 2007) or by the production of particulate filled or fiber reinforced composites (Bax & Müssig, 2008; Bhat, Gulgunje, & Desai, 2008; Bleach, Nazhat, Tanner, Kellomäki, & Törmälä, 2002; Gorna, Hund, Vucak, Grohn, & Wegner, 2008; Kuan, Kuan, Ma, & Chen, 2008; Murariu, Ferreira, Degee, Alexandre, & Dubois, 2007; Murariu et al., 2008; Paul et al., 2003; Pluta, Jeszka, & Boiteux; Pluta et al., 2007; Sobkowicz, Feaver, & Dorgan, 2008; Wang, Zhang, Ma, & Fang, 2008). Although PLA has several drawbacks (low heat deflection temperature, fast physical aging, water sensitivity, brittleness), it also has considerable advantages compared to fossil fuel based polymers. Among others it can be produced from renewable resources thus its application does not generate supplementary CO_2 emission, it is recyclable and compostable in industrial composts, and its properties can be modified and adjusted to a large number of applications in various ways. Increasing production capacity decreases its price thus PLA may represent a reasonable alternative to commodity polymers in several application areas. Calcium sulfate forms as a byproduct during the purification of the lactic acid monomer, thus it is reasonable to attempt the use of this mineral for the modification of PLA. Such an approach may result in a reasonable utilization of the byproduct and allow the preparation of a new material (Mishra & Shimpi, 2007; Murariu et al., 2007, 2008; Pluta et al., 2007; Sobkowicz et al., 2008). As it has been shown elsewhere (Sobkowicz et al., 2008), the preparation of PLA/$CaSO_4$ composites satisfies two of the twelve principles

* Corresponding author at: Institute of Materials and Environmental Chemistry, Chemical Research Center, Hungarian Academy of Sciences, H-1525 Budapest, P.O. Box 17, Hungary. Tel.: +36 1 4632015; fax: +36 1 4633474.
E-mail address: bpukanszky@mail.bme.hu (B. Pukánszky).

0144-8617/$ – see front matter © 2012 Elsevier Ltd. All rights reserved.
http://dx.doi.org/10.1016/j.carbpol.2012.04.005

of green chemistry, i.e. the use of renewable feedstock and the prevention of waste formation. The use of gypsum as a filler for PLA decreases the cost of the polymer and makes it competitive with traditional petrochemical polymers. However, further study is needed to determine structure–property correlations, deformation and failure behavior, performance and potential application areas of this relatively new composite (Murariu et al., 2007).

In a recent study we prepared PLA composites containing uncoated $CaSO_4$ and the same filler coated with stearic acid, and determined their structure and properties (Molnár, Móczó, Murariu, Dubois, & Pukánszky, 2009). We found that surface modification changes all properties drastically, which indicates the importance of interfacial interactions in the determination of composite properties. Moreover, with specifically designed experiments we found that stearic acid dissolves in PLA and plasticizes the polymer around the particles which can lead to local plastic deformation. We assumed that the dominating micromechanical deformation mechanism is debonding, i.e. the separation of the matrix and the filler at the interface, which justifies the increased importance of interfacial interactions. However, we did not have direct evidence for this assumption. Finally, we also found widely deviating points in some of our correlations, which were difficult or impossible to understand. The compression molding of stiff PLA, which becomes even stiffer upon filling, proved to be a difficult task and we speculated that inappropriate sample preparation conditions might have resulted in stress concentrations or other defects in the samples leading to the deviations observed.

Taking into consideration all these questions, the goal of the present study was to focus more on interfacial interactions and micromechanical deformation processes in PLA/$CaSO_4$ composites. The samples were homogenized by extrusion and specimens were prepared by injection molding this time. Less attention was paid to structure, but more effort was spent on the surface characterization of the filler, on the estimation of interfacial adhesion and on deformation processes. Similarities and differences caused by the dissimilar conditions are pointed out and the practical consequences are discussed in the paper.

2. Experimental

The PLA used in the experiments was obtained from NatureWorks (USA). The selected grade (Ingeo 4032D, M_n = 88 500 g/mol and M_w/M_n = 1.8) is recommended for extrusion. The polymer (<2% D isomer) has a density of 1.24 g/cm^3, while its MFI is 3.9 g/10 min at 190 °C and 2.16 kg load. The CAS-20-4 calcium sulphate filler used was supplied by the United States Gypsum Co. (USA). The filler, manufactured from high purity gypsum rock using controlled calcination and fine grinding, has a volume average particle size of 4.4 μm, specific gravity of 2.96 g/cm^3 and calcium sulfate content >99%. The filler was surface coated with 1.5 wt% stearic acid resulting in monolayer coverage (Molnár et al., 2009) in order to modify interfacial interactions. Coating was carried out at 120 °C and 100 rpm for 10 min in a Haake Rheomix 600 mixer fitted with blades for dry-blending. The $CaSO_4$ content of the PLA composites, both with coated and uncoated fillers, was changed from 0 to 30 vol% in 5 vol% steps.

The particle size and particle size distribution of the filler was determined with a Malvern Mastersizer 2000, while its specific surface area with an Autosorb 1 (Quantachrome, USA) apparatus. The surface characteristics of the fillers were studied by inverse gas chromatography (IGC). The fillers were aggregated in methanol then the dried samples were grinded and sieved. The size of the grinded filler particles covered a wide range; the fraction between 400 and 800 μm size was used for the filling of the column. Columns were conditioned at 140 °C for 16 h and measurements were done at different temperatures (90–120 °C) with the injection of various n-alkanes and polar solvents (tetrahydrofurane, diethyl ether, ethyl acetate, chloroform).

Both poly(lactic acid) and the fillers were dried in a vacuum oven before composite preparation (110 °C for 4 h and 120 °C for 2 h, respectively). The components were homogenized using a Brabender DSK 42/7 twin screw compounder at 205–205–210 °C and 30 rpm followed by granulation. Standard specimens (ISO 527 1A) were produced by injection molding (Demag IntElect 50/330-100) at 200–210–220–230 °C barrel and 40 °C mold temperature, 550 bar injection and 500 bar holding pressure at 35 s holding time. All specimens were kept in a room with controlled temperature and humidity (23 °C and 50%) for at least one week prior further testing.

The possible crystallinity of the samples was checked by X-ray diffraction (XRD) using a Phillips PW 1830/PW 1050 apparatus with CuK_α radiation at 40 kV and 35 mA anode excitation. XRD spectra were registered between 5 and 35°2θ angles. Crystallinity was determined also by differential scanning calorimetry using a Perkin Elmer DSC 7 apparatus. Only one heating run was done on 5 mg samples with a heating rate of 10 °C/min.

The filler was coated with 1.5 wt% surfactant as described in a previous paragraph. The amount of bonded stearic acid on the filler surface prior to compounding and in the composite was compared using FTIR-DRIFT spectroscopy. In order to separate the coated filler from the PLA matrix, 11.3 g of the composite containing 25 vol% (5 g) of coated filler was stirred for 5 h in 100 ml of chloroform and dichloromethane respectively. The filler was analyzed following filtration and drying. For the sake of comparison, the same method was applied to 5 g of the coated filler, while the neat uncoated and coated fillers were used as references.

Mechanical properties were characterized by tensile testing on standard 4 mm thick ISO 527 1A specimens using an Instron 5566 apparatus. Stiffness (E) was determined at 0.5 mm/min cross-head speed and 115 mm gauge length. Tensile strength (σ), and elongation-at-break (ε) were calculated from force vs. deformation traces measured on the same specimens at 5 mm/min cross-head speed. Micromechanical deformation processes were studied by volume strain (VOLS) and acoustic emission (AE) measurements. Volume strain was determined by the measurement of changes in the dimension of the specimen also in a lateral direction; we assumed that changes in the other lateral direction are similar. A Sensophone AED 40/4 apparatus was used to record and analyze acoustic signals during tensile tests. Both standard and instrumented impact tests were carried out to characterize fracture resistance. Impact testing was done according to the ISO 179 standard on 80 × 10 × 4 mm specimens using a Ceast Resil 5.5 apparatus (2 mm notch, 62 mm span, 4 J hammer, 2.9 m/s). The particle characteristics of $CaSO_4$ and the structure, as well as the deformation mechanism of the composites were studied by scanning electron microscopy, SEM (JEOL JSM-6380 LA). Micrographs were recorded on both impact and tensile fracture surfaces.

3. Results and discussion

The morphology of PLA/$CaSO_4$ composites is relatively complicated. The polymer can crystallize, but the rate of crystallization is rather slow thus under the conditions of normal processing operations it remains mostly amorphous; its crystalline content is very small. Besides crystalline structure, the distribution of the filler in the matrix, i.e. the possible formation of aggregates, especially at large filler loadings, is also an important issue. The filler might influence also interphase formation and the mobility of the polymer molecules. We investigated these questions in our previous study in detail (Molnár et al., 2009). We found that crystallinity is negligible and additional measurements done in this study by XRD and DSC confirmed this result. Very little aggregation was found earlier in spite of the presence of a fraction of small particles. The most

Table 1
Effect of filler content on the glass transition temperature of PLA.

Filler content (vol%)	0	5	10	15	20	25	30
Tg (°C)							
Coated	66.3	66.2	65.7	65.6	65.1	65.6	64.6
Uncoated	66.3	66.3	66.2	66.4	66.5	66.4	66.3

important structural aspect was the plasticizing effect of stearic acid on PLA. Taking into consideration previous results and supporting information obtained in this study we refrain from the detailed discussion of structure and focus mostly on properties, surface characteristics, interfacial adhesion and micromechanical deformations. Consequences for practice are discussed in the final section of the paper.

3.1. Properties

The mechanical properties of the PLA/$CaSO_4$ composites studied is plotted against filler content in Fig. 1. Stiffness increases steeply with increasing filler content and reaches almost 8 GPa at 30 vol%. The effect of surface modification is very small; the stiffness of the composites containing the coated filler is only slightly smaller than the modulus of materials containing the uncoated filler. This result is in complete agreement with earlier experience showing that neither interaction nor structure influence stiffness much (Parrinello, 1991; Pukánszky, 1992). The slight decrease of stiffness upon coating might be the result of decreased interfacial interaction or the plasticizing effect of the stearic acid. In the first case the debonding of large particles may occur already at the very small deformations of the modulus measurement. Plasticization on the other hand should affect the glass transition temperature (T_g) of the matrix polymer. It is worthy to note that similarly to the composition dependence of stiffness, slight difference could be observed in the glass transition temperature of the composites (see Table 1). As determined from the DSC traces of the composites, T_g shifted to lower temperatures confirming the minor plasticizing effect of stearic acid in PLA. If plasticization is the reason of decreased stiffness, the effect is slight, probably due to the constraint of the larger specimen thickness, which hinders plastic deformation. Finally, the composition dependence of stiffness indicates the complete lack of structural effects, the correlation agrees well with predictions (Nielsen, 1974; Wypych, 1999), as shown by the broken line in Fig. 1a. The composition dependence of modulus was predicted with the Lewis–Nielsen equation (Eqs. (1)–(4))

$$E = E_m \frac{1 + AB\varphi_f}{1 - B\Psi\varphi_f} \quad (1)$$

$$A = \frac{7 - 5\nu_m}{8 - 10\nu_m} \quad (2)$$

$$B = \frac{E_f/E_m - 1}{E_f/E_m + A} \quad (3)$$

$$\Psi = 1\left(\frac{1 - \varphi_f^{\max}}{\varphi_f^{\max 2}}\right)\varphi_f \quad (4)$$

where E, E_m (3.6 GPa) and E_f (63.9 GPa) are the Young's modulus of the composite, matrix and filler (Sharpe & Cork, 2006), respectively, ν_m (0.35) is the Poisson's ratio of the matrix and φ_f^{max} (0.64) is maximum packing fraction (Nielsen, 1974). Orientation does not play a role because the aspect ratio of the filler is close to 1, while aggregation probably does not occur either in accordance with previous results.

The composition dependence of tensile strength is presented in Fig. 1b for the two series of composites. The strength of the

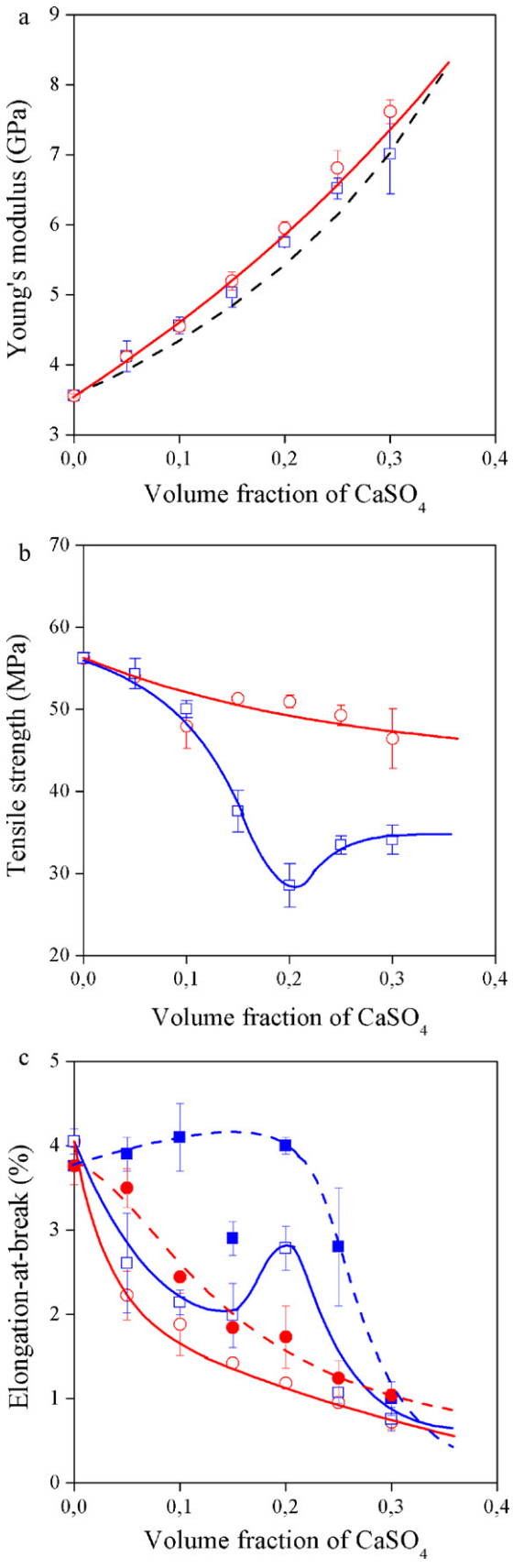

Fig. 1. Effect of surface coating and filler content on tensile properties of PLA/$CaSO_4$ composites; (a) tensile modulus (○) uncoated, (□) coated filler, —— prediction (Eqs. (1)–(4)); (b) tensile strength (○) uncoated, (□) coated filler; (c) deformability (○, ●) uncoated, (□, ■) coated filler; effect of technology and specimen thickness: ——— 4 mm, injection molded, —— 1 mm compression molded.

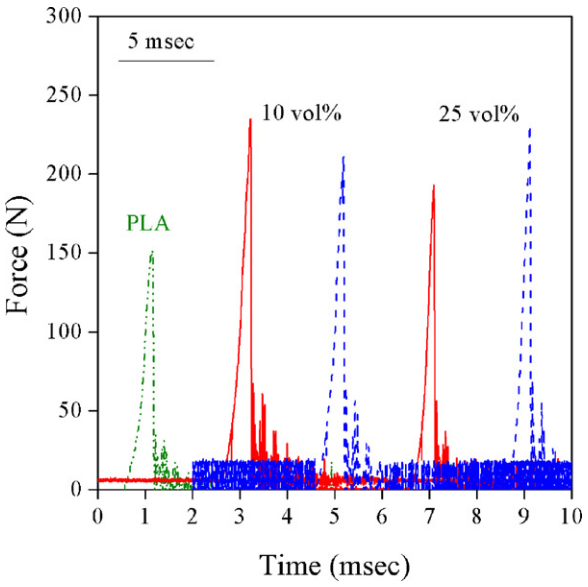

Fig. 2. Instrumented impact testing of PLA/$CaSO_4$ composites, effect of surface coating and filler content; ·-·-·-·- PLA, ——— uncoated filler, —— coated filler.

composites containing the uncoated filler decreases only slightly. This result agrees well with previous findings and indicates good interaction between the filler and the polymer matrix. Much more complicated is the composition dependence of strength for composites prepared with the coated filler. Strength decreases quite significantly with increasing filler content and shows a minimum at 20 vol% $CaSO_4$ content which is difficult to explain. The large decrease in strength indicates weak interfacial adhesion and probably easy debonding. The minimum might result from the combined effect of plasticization, size constraint and changing interparticle distance. The deformability of the composites changes similarly, as a function of composition as presented in Fig. 1c, in which the results obtained on 1 mm thick compression molded plates are also included as reference. In complete accordance with the composition dependence of strength, elongation-at-break shows a maximum at 20 vol% filler content for the injection molded specimens. Obviously, the combination of the factors mentioned above results in a maximum in deformability and a minimum in strength in this range of filler loading. It also should be noted that elongation-at-break is very small for composites containing the uncoated filler and it is only marginally larger for composites prepared with the coated filler, though deformability remains below 4% in all cases. Specimen thickness has a similar effect on composites containing both the coated and the uncoated filler, but coating has a much larger effect at 1 mm thickness. Apparently plasticization and/or local plastic deformation influence deformability much more at smaller constraint.

Limited fracture resistance is one of the drawbacks of PLA. Combination with fillers might increase (Bartczak, Argon, Cohen, & Weinberg, 1999; Dubnikova, Berezina, & Antonov, 2002; Razi & Raman, 2000; Wang, Wu, Ye, & Zeng, 2003; Zuiderduin, Westzaan, Huétink, & Gaymans, 2003) or decrease (Dubnikova et al., 2002; Razi & Raman, 2000; Zebarjad, Tahani, & Sajjadi, 2004) impact strength depending on the extent of plastic deformation initiated by the filler. Considering the differences in deformability and strength (see Fig. 1b and c) we expected large difference in the fracture behavior of composites containing the coated and the uncoated filler, respectively. A few selected force vs. time traces recorded during instrumented impact testing are presented in Fig. 2. The traces are very similar to each other; considerable differences cannot be established without quantitative analysis. The presence of the filler increases the maximum force, i.e. the critical stress intensity factor for fracture initiation. Fracture energy seems to be more or less the same for the two series of composites. The larger force and area measured at 25 vol% content of the coated filler indicates some increase in plastic deformation, but this is much below the extent expected. The lack of pronounced effect of coating on fracture resistance is strange and might be explained with the high speed (2.9 m/s) of testing and the size constraint of the large specimens. We may conclude, however, that the coating of the filler changes interfacial interaction and also the extent of plastic deformation thus a more thorough study of these factors is needed for the understanding of the behavior of PLA/$CaSO_4$ composites.

Table 2
Surface characteristics of the $CaSO_4$ fillers studied.

Filler	Surface tension,[a] γ_s^d (mJ/m^2)	Acid–base constants	
		K_a	K_d
Uncoated	79.8	0.10	0.54
Coated	21.6	0.37	0.52

[a] Determined at 120 °C.

3.2. Surface characterization

In the absence of coupling, i.e. covalent bonds, between the matrix and the filler, interfacial interactions are created by secondary bonds. The character and strength of interactions can be estimated quite well by the proper characterization of the surface. Surface properties are often determined by inverse gas chromatography, which allows the determination of both the apolar, dispersion and the polar, specific components of interaction (Comard, Calvet, Balard, & Dodds, 2004; Comte, Calvet, Dodds, & Balard, 2005; Mukhopadhyay & Schreiber, 1995; Panzer & Schreiber, 1992). The dispersion component of surface tension is determined by the method of Dorris and Gray (1980) using retention volumes obtained by the injection of n-alkanes onto the column, the packing of which is the filler itself. Because of the large surface energy of $CaSO_4$ even the determination of the dispersion component is not easy, the probe does not elute at room temperature, thus the measurement is done at higher temperatures. The specific component of interaction can be characterized by the donor (DN) and acceptor (AN) numbers of Drago, Vogel, and Needham (1971) or Gutmann (1978). The injection of polar solvents with known AN and DN numbers allows the determination of the enthalpy change of adsorption and from its temperature dependence the determination of the acid–base constants K_a and K_d (Gutmann, 1978).

The surface characteristics of the two fillers studied are collected in Table 2. The dispersion component of surface energy is relatively large compared to $CaCO_3$ that has a value of about 65 mJ/m^2 at 50 °C and 45 mJ/m^2 at 120 °C (Fekete, Móczó, & Pukánszky, 2004). Surface tension decreases considerably upon coating, instead of the 80 mJ/m^2 measured for the uncoated filler we obtain 21.6 mJ/m^2 after coating. Both values mentioned were determined at 120 °C. The dispersion component of surface tension does not give information about specific interactions, although the carbonyl group of PLA is definitely capable of forming strong bonds, which probably lead to strong interfacial adhesion. IGC measurements indicate that the surface of the fillers is amphoteric in character, but it is much more basic than acidic. Acidity increases upon surface treatment, which is not very surprising considering that coating was done with stearic acid. These values explain both the strong interaction between the uncoated filler and the polymer, and the increase in acidity with coating indicates the presence of free or weakly bonded stearic

acid, which, on the other hand, explains the dissolution and the plasticization effect of this surfactant in PLA.

3.3. Interfacial adhesion

The strength of interfacial adhesion can be estimated in several ways in particulate filled composites. If we know the components of surface energy, the reversible work of adhesion can be calculated quantitatively as

$$W_{AB} = 2(\gamma_1^d \gamma_2^d)^{1/2} + n^{ab} f \Delta H^{ab} \quad (5)$$

where γ_1^d and γ_2^d are the dispersion component of the surface tension for components 1 and 2, respectively, f is a correction factor close to unity, n^{ab} is the number of interacting acid–base sites located on the surface, and ΔH^{ab} is the enthalpy related to acid–base interaction. Recently an approach was developed to determine the strength of interfacial adhesion from acoustic emission measurements (Renner, Móczó, Vörös, & Pukánszky, 2010). The basis of the approach is Eq. (6), which defines debonding stress as

$$\sigma^D = -C_1 \sigma^T + C_2 \left(\frac{E W_{AB}}{R} \right)^{1/2} \quad (6)$$

where σ^D and σ^T are debonding and thermal stresses, respectively, E the Young's modulus of the matrix, W_{AB} the reversible work of adhesion, R the radius of the particles, while C_1 and C_2 are geometric constants related to the debonding process. If we know the parameters of the equation, which were calculated from measurements done on polymer/filler pairs with known characteristics (E, R, W_{AB}), and know the stiffness of the matrix and the size of the particles, which we usually do, we can calculate the strength of adhesion, which we term F_a instead of W_{AB} in order to differentiate the approach used for determination. Finally, the strength of interfacial adhesion can be also estimated from the composition dependence of composite strength if the dominating deformation mechanism is debonding. The dependence of tensile strength on filler content can be expressed as

$$\sigma_T = \sigma_{T0} \lambda^n \frac{1-\varphi}{1+2.5\varphi} \exp(B\varphi) \quad (7)$$

where σ_T and σ_{T0} are the true tensile strength ($\sigma_T = \sigma\lambda$ and $\lambda = L/L_0$) of the composite and the matrix, respectively, n is a parameter expressing the strain hardening tendency of the matrix, φ is the volume fraction of the filler and B is related to its relative load-bearing capacity, i.e. to the extent of reinforcement, which depends on interfacial interaction. We can write Eq. (7) in linear form

$$\ln \sigma_{Tred} = \ln \frac{\sigma_T (1+2.5\varphi)}{\lambda^n (1-\varphi)} = \ln \sigma_{T0} + B\varphi \quad (8)$$

and plotting the natural logarithm of the reduced tensile strength of the composite against filler content should result in a linear correlation, the slope of which is proportional to the strength of interaction. In Fig. 3 the strength of the two series of composites is plotted against filler content in the form indicated by Eq. (8). We obtain linear correlations indeed with considerably different slopes which clearly show the difference in the strength of interfacial adhesion.

The results obtained with the three different approaches are compiled in Table 3 for the two fillers. We can see that in spite of the dissimilar approaches the final results are the same. Even the absolute values are similar for adhesion obtained from thermodynamic calculations and acoustic emission measurements, but parameter B determined from the composition dependence of tensile strength also shows that the strength of interfacial adhesion is significantly larger in composites containing the uncoated filler than in those prepared with coated $CaSO_4$. The results are consistent and indicate

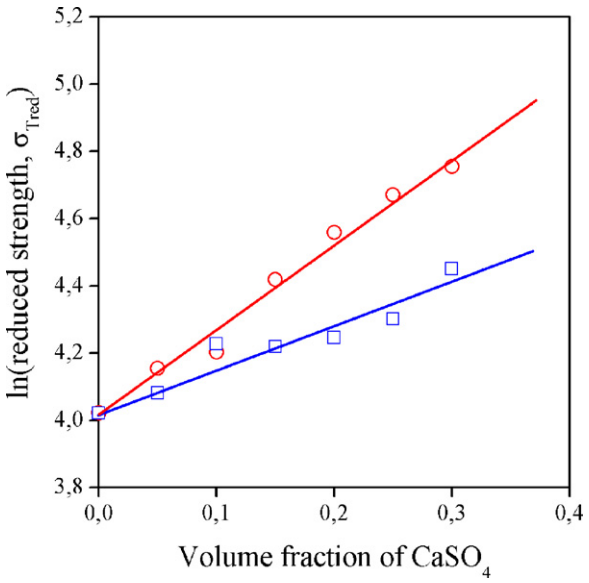

Fig. 3. Effect of surface coating on the reinforcing effect of the filler in PLA/$CaSO_4$ composites; (○) uncoated, (□) coated filler.

that debonding is facilitated by coating. On the other hand, easier debonding does not necessarily mean larger plastic deformation and does not give information about the possible plasticizing effect of stearic acid in PLA.

3.4. Micromechanical deformations

External load induces stress concentration around heterogeneities in particulate filled composites. Local stress maxima initiate local deformation processes and their detection gives valuable information about the mechanism of the processes and often also about the performance of the material. Debonding results in the formation of voids which increases the volume of the specimen. However, detectable volume increase starts only after the considerable plastic deformation of the material around the heterogeneities (Renner, Yang, Móczó, Choi, & Pukánszky, 2005). The volume increase of three specimens is compared in Fig. 4a together with the corresponding stress vs. strain traces. We can see that volume increases more or less linearly at small deformations with very similar slopes for the three materials. The increase is the result of Poisson's ratio being different from 0.5. Larger differences can be detected among the materials above 1.0% elongation. Apparently a decrease of volume increase seems to occur in neat PLA, which is usually an indication of inhomogeneous deformation and yielding. The uncoated filler with strong interfacial adhesion fails before volume starts to increase. This may indicate the complete absence of debonding, but more probably the immediate, catastrophic failure of the specimen after the separation of the interfaces. Large volume increase is observed in the composite containing the coated filler, which is in complete agreement with the large deformability and small strength of this material. Debonding occurs at lower stress

Table 3
Effect of surface coating on matrix/filler adhesion determined with three independent methods in PLA/$CaSO_4$ composites.

Filler	Interfacial adhesion determined from		
	Surface characteristics W_{AB} (mJ/m^2)	Acoustic emission F_a (mJ/m^2)	Tensile strength Parameter B
Uncoated	243	211	2.56
Coated	121	134	1.24

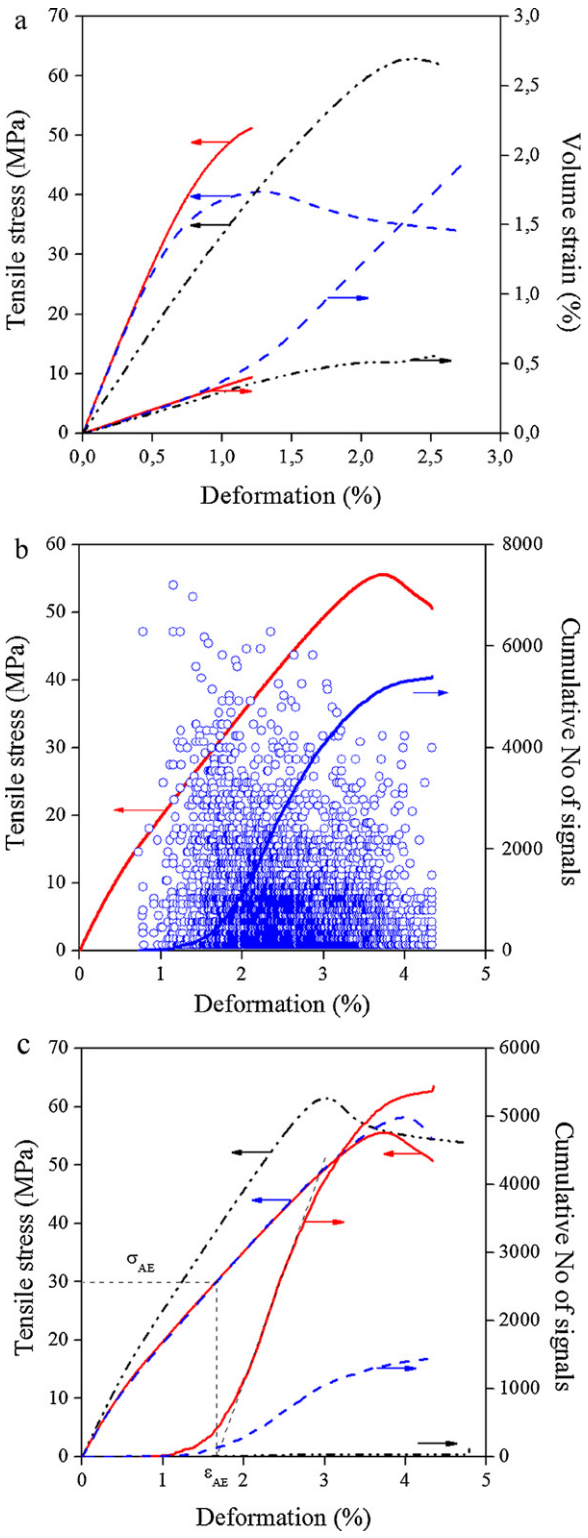

Fig. 4. Results of the volume increase and acoustic emission measurements: (a) volume increase, filler content: 20 vol%, ·-·-·-· PLA, ——— uncoated filler, —– coated filler; (b) acoustic emission measurement (5 vol% coated filler) (○) individual acoustic signals; (c) acoustic activity of PLA and its composites. Filler content: 5 vol%, ·-·-·-· PLA, ——— uncoated filler, —– coated filler.

which can be explained by the weaker adhesion due to the surface treatment of the filler. As we have shown earlier, the PLA can dissolve the stearic acid form the surface of $CaSO_4$ (Molnár et al., 2009), but dissolution is never complete; some surfactant remains on the surface which results in weaker interaction compared to the neat filler. The fact that a certain, lower extent of surface coverage is still present in the composites was demonstrated by DRIFT measurement of coated fillers extracted from the composite after dissolution of the matrix; these results however are not listed here. Considering all these factors, we might conclude that the effect of debonding, stearic acid plasticization and changing particle distance results in this large volume increase.

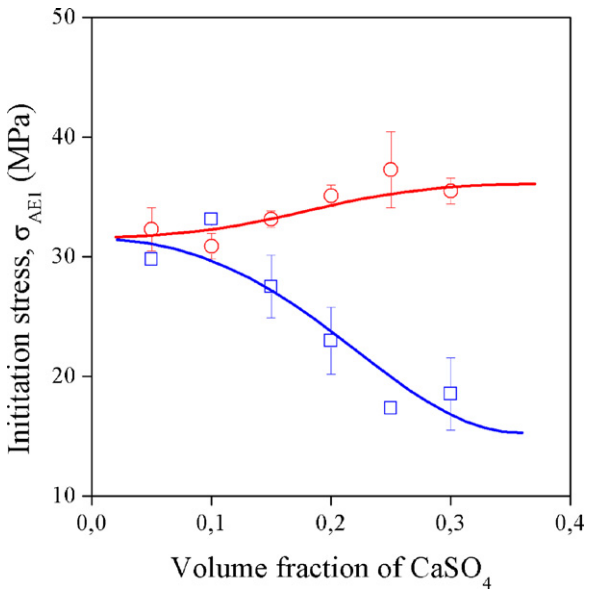

Fig. 5. Effect of filler content and surface coating on the initiation stress for debonding determined by acoustic emission in PLA/$CaSO_4$ composites; (○) uncoated, (□) coated filler.

The result of acoustic emission measurement done on the composite containing the uncoated filler in 5 vol% indicates that considerable number of acoustic events occur in the material during deformation (Fig. 4b). Individual acoustic events are indicated with small circles in the figure; their amplitude changes between the threshold value of 20 dB and a maximum around 80 dB. It is quite difficult to draw much conclusion from individual signals thus we plot also the cumulative number of signals in the figure together with the stress vs. strain trace for comparison. The *S* shape of the cumulative number of signals vs. elongation correlation is typical for debonding (Renner et al., 2005). We can also determine a characteristic stress value from such traces indicating the initiation of debonding (σ_{AE}, see Fig. 4c). This value can be and was used for the calculation of the strength of interfacial adhesion (F_a, Table 3) according to the second approach described above (see Eq. (2), σ^D).

Correlations of the cumulative number of signals are compared in Fig. 4c for three materials, for the PLA and for composites containing the uncoated and coated $CaSO_4$ filler in 5 vol%, respectively. Hardly any sound is detected in the matrix polymer indicating that it deforms mainly elastically and by shear yielding that do not give sound. The shape of the cumulative number of signal correlations is similar for the two composites; the only difference is in the number of signals, which is much smaller in the composite containing the coated filler. The small number of signals may be the result of fewer acoustic events, but the strength of adhesion was also shown to influence the number of signals and/or their detection. Considerable local yielding and changing matrix properties as a result of plasticization may also contribute to the smaller number of acoustic emission signals.

The characteristic stress value related to the appearance of acoustic signals, which we assign to the initiation of debonding, is plotted against filler content in Fig. 5 for the two composite series. Composition dependence differs considerably for the two

types of fillers. Characteristic stress increases slightly with filler content for composites containing uncoated $CaSO_4$. Such a behavior was explained before with the effect of interacting stress fields leading to a decrease of local stresses (Pukánszky & Vörös, 1996). On the other hand, coating obviously facilitates debonding. However, the composition dependence cannot be explained solely with this effect, since the strength of interaction is the same at all filler contents. Obviously some other factor or factors also contribute to the initiation of debonding. We may assume that local deformation, changing matrix properties due to the plasticizing effect of stearic acid and changes in particle distance all contribute to the decrease of debonding stress.

3.5. Discussion

The results presented above clearly prove the important role of interfacial adhesion on the deformation and failure behavior of PLA/$CaSO_4$ composites. The coating of the filler surface with stearic acid does not influence the stiffness of the composites much, as expected, but results in a considerable decrease in composite strength. The dominating micromechanical deformation is clearly debonding, which could be proved both by volume strain and acoustic emission measurements. Stearic acid treatment increases the deformability of the composites and facilitates debonding. However, the extremes in the composition dependence of strength and elongation-at-break indicate the effect of additional factors, almost certainly the role of local deformations which depend on composition, but also on the presence or absence of stearic acid on the surface of the filler. Although the overall homogeneity of the composites is satisfactory as indicated by several results, local inhomogeneity may also influence macroscopic properties.

Although electron micrographs cannot supply unassailable evidence about the local deformation processes occurring around particles, they can at least offer some information supporting our assumptions. The fracture surface of a specimen created during tensile testing is shown in Fig. 6a; the composite contained 30 vol% uncoated filler. The surface shows all the characteristics of PLA/$CaSO_4$ composites prepared with uncoated particles. Several large and a large number of small particles can be seen in the figure. Considering the large filler content, the homogeneity of the sample is reasonable and the fracture surface is smooth indicating limited extent of plastic deformation. A completely different view is offered by the fracture surface of the composite containing the same amount of filler, but prepared with coated $CaSO_4$ (Fig. 6b). The large particles are visible here too, but the presence of smaller ones is obscured by the large extent of plastic deformation around the large particles. The large holes around these particles also support our conclusions about facilitated debonding (Fig. 1b), void formation (Fig. 4a) and large plastic deformation. Although based on these micrographs we do not dare to draw farfetched conclusions, we may safely say that local deformation processes play an important role in the determination of the ultimate properties of PLA/$CaSO_4$ composites. The role of increased local plastic deformation is further supported by Fig. 7 in which the toughness of the composites calculated from tensile characteristics ($\sigma \Delta L/L_0$) is plotted against filler content. The difference in the toughness of the two sets of composites is not large, but definite thus verifying our arguments presented above.

To further emphasize the correlation between local processes and macroscopic properties, we plotted composite strength against the characteristic stress indicating the initiation of debonding which was determined from acoustic emission experiments (Fig. 8). The correlation is unambiguous proving that local processes determine the performance of the composite indeed. However, a closer scrutiny reveals that the points for the composite prepared with the uncoated filler cover a very narrow range, on the one hand, while some points considerably deviate from the general tendency in the other series, for composites containing the coated filler. These deviations clearly prove that another factor or process also plays a role in the determination of composite strength and we believe that this

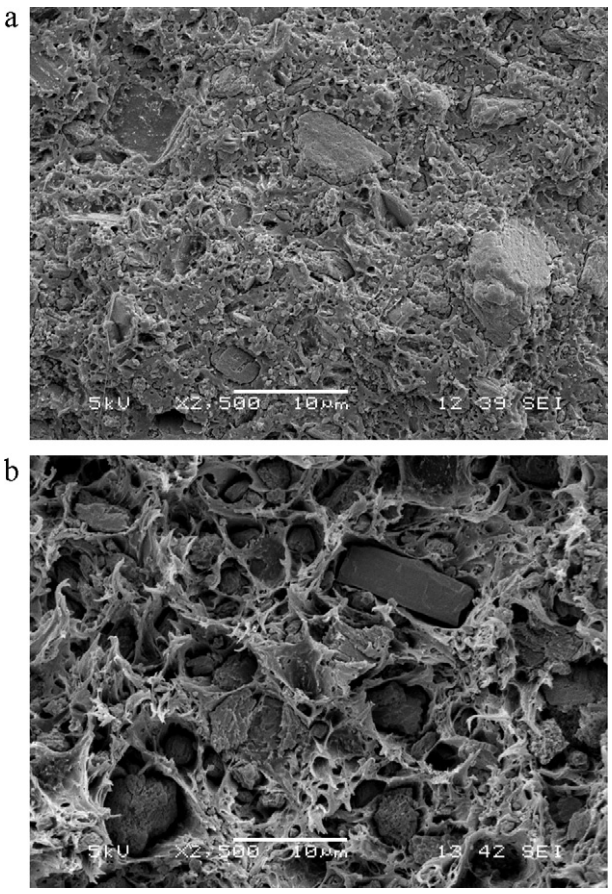

Fig. 6. Scanning electron micrographs recorded on the surface created by the failure of the specimen during tensile testing. Effect of surface coating. Filler content: 30 vol%. (a) Uncoated; (b) coated $CaSO_4$.

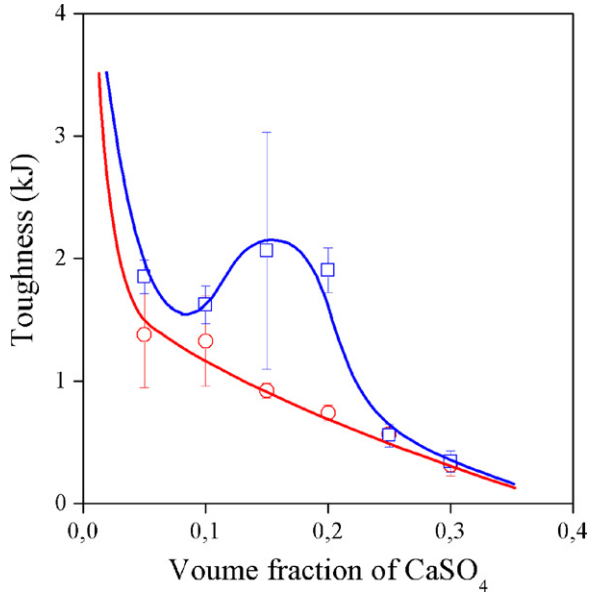

Fig. 7. Effect of coating on the toughness ($\sigma \Delta L/L_0$) of PLA/$CaSO_4$ composites prepared with uncoated and coated filler, respectively. (○) Uncoated, (□) coated filler.

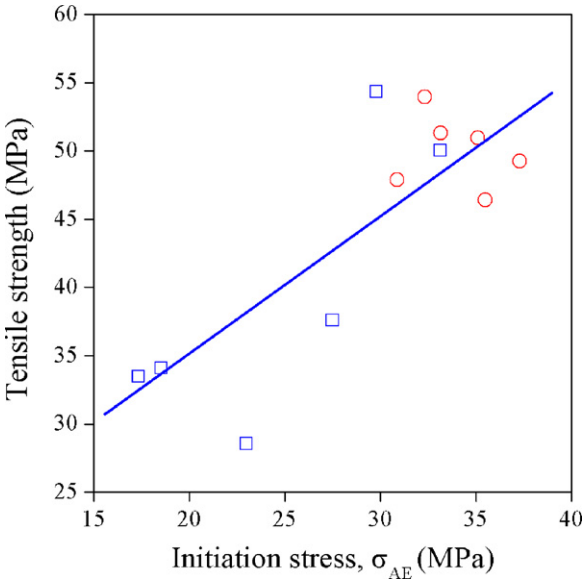

Fig. 8. Correlation between composite strength and the initiation stress of debonding in PLA/$CaSO_4$ composites. (○) Uncoated, (□) coated filler.

is local plastic deformation the extent of which depends also on the local distribution of the particles. The coating of the filler facilitates debonding through decreasing the strength of interaction, but also promotes plastic deformation by changing matrix properties.

4. Conclusions

PLA/$CaSO_4$ composites were prepared from uncoated and stearic acid coated filler particles. The study of the properties as well as deformation and failure characteristics of injection molded specimens proved the crucial role of interfacial interactions in the determination of composite properties. Interfacial adhesion was estimated with three independent methods all proving that adhesion is twice as strong in composites prepared with the uncoated particles than in those containing the coated filler. Coating also changes local deformation processes. Although debonding is the dominating micromechanical deformation process in all composites, local plastic deformation is larger around coated particles. The extent of this deformation depends very much also on the local distribution of particles. The final properties and performance of the composites depend unambiguously on the micromechanical deformation processes occurring during loading, on debonding and the subsequent plastic deformation. Stearic acid used for the coating of the filler seems to dissolve in the polymer and locally change its properties.

Acknowledgements

The research on heterogeneous polymer systems was partly financed by the National Scientific Research Fund of Hungary (OTKA Grant nos. K 68748 and F 68579), we appreciate the support very much. CIRMAP thanks the Belgian Federal Government Office Policy of Science (SSTC) for general support in the frame of PAI-6/27 and Region Wallone in the frame of OPT²MAT Program of Excellence.

References

Auras, R., Harte, B., & Selke, S. (2004). An overview of polylactides as packaging materials. *Macromolecular Bioscience*, *4*, 835–864.

Bartczak, Z., Argon, A. S., Cohen, R. E., & Weinberg, M. (1999). Toughness mechanism in semi-crystalline polymer blends: II. High-density polyethylene toughened with calcium carbonate filler particles. *Polymer*, *40*, 2347–2365.

Bax, B., & Müssig, J. (2008). Impact and tensile properties of PLA/Cordenka and PLA/flax composites. *Composites Science and Technology*, *68*, 1601–1607.

Belgacem, M. N., & Gandini, A. (2008). *Monomers, polymers and composites from renewable resources*. Amsterdam: Elsevier.

Bhat, G. S., Gulgunje, P., & Desai, K. (2008). Development of structure and properties during thermal calendering of polylactic acid (PLA) fiber webs. *Express Polymer Letters*, *2*, 49–56.

Bleach, N. C., Nazhat, S. N., Tanner, K. E., Kellomäki, M., & Törmälä, P. (2002). Effect of filler content on mechanical and dynamic mechanical properties of particulate biphasic calcium phosphate–polylactide composites. *Biomaterials*, *23*, 1579–1585.

Comard, M. P., Calvet, R., Balard, H., & Dodds, J. A. (2004). The influence of polymer impregnation ratios on the surface properties of fumed silicas as determined by inverse gas chromatography. *Colloids and Surfaces A-Physicochemical and Engineering Aspects*, *232*, 269–274.

Comte, S., Calvet, R., Dodds, J. A., & Balard, H. (2005). Surface properties of low specific surface powders using inverse gas chromatography. *Powder Technology*, *157*, 39–47.

Dorris, G. M., & Gray, D. G. (1980). Adsorption of normal-alkanes at zero surface coverage on cellulose paper and wood fibers. *Journal of Colloid and Interface Science*, *77*, 353–362.

Drago, R. S., Vogel, G. C., & Needham, T. E. (1971). Four-parameter equation for predicting enthalpies of adduct formation. *Journal of the American Chemical Society*, *93*, 6014–6026.

Dubnikova, I. L., Berezina, S. M., & Antonov, A. V. (2002). The effect of morphology of ternary-phase polypropylene/glass bead/ethylene–propylene rubber composites on the toughness and brittle-ductile transition. *Journal of Applied Polymer Science*, *85*, 1911–1928.

Evans, J. (2011). Alternative feedstocks. How viable? *Plastics Engineering*, *67*, 12–17.

Fekete, E., Móczó, J., & Pukánszky, B. (2004). Determination of the surface characteristics of particulate fillers by inverse gas chromatography at infinite dilution: A critical approach. *Journal of Colloid and Interface Science*, *269*, 143–152.

Gandini, A. (2008). Polymers from renewable resources: A challenge for the future of macromolecular materials. *Macromolecules*, *41*, 9491–9504.

Gorna, K., Hund, M., Vucak, M., Grohn, F., & Wegner, G. (2008). Amorphous calcium carbonate in form of spherical nanosized particles and its application as fillers for polymers. *Materials Science and Engineering A-Structural Materials Properties Microstructure and Processing*, *477*, 217–225.

Gu, S. Y., Zhang, K., Ren, J., & Zhan, H. (2008). Melt rheology of polylactide/poly(butylene adipate-co-terephthalate) blends. *Carbohydrate Polymers*, *74*, 79–85.

Gutmann, V. (1978). *The donor–acceptor approach to molecular interactions*. Plenum Press: New York.

Hirata, M., & Kimura, Y. (2008). Thermo mechanical properties of stereoblock poly(lactic acid)s with different PLLA/PDLA block compositions. *Polymer*, *49*, 2656–2661.

Ho, C. H., Wang, C. H., Lin, C. I., & Lee, Y. D. (2008). Synthesis and characterization of TPO-PLA copolymer and its behavior as compatibilizer for PLA/TPO blends. *Polymer*, *49*, 3902–3910.

Kuan, C.-F., Kuan, H.-C., Ma, C.-C. M., & Chen, C.-H. (2008). Mechanical and electrical properties of multi-wall carbon nanotube/poly(lactic acid) composites. *Journal of Physics and Chemistry of Solids*, *69*, 1395–1398.

Li, B., Chen, S. C., Qiu, Z. C., Yang, Q. K. K., Tang, S. P., Yu, W. J., et al. (2008). Synthesis of poly(lactic acid-b-p-dioxanone) block copolymers from ring opening polymerization of p-dioxanone by poly(L-lactic acid) macroinitiators. *Polymer Bulletin*, *61*, 139–146.

Lindblad, M. S., Liu, Y., Albertsson, A. C., Ranucci, E., & Karlsson, S. (2002). Polymers from renewable resources. *Degradable Aliphatic Polyesters*, *157*, 139–161.

Mert, O., Doganci, E., Erbil, H. Y., & Dernir, A. S. (2008). Surface characterization of poly(L-lactic acid)-methoxy poly(ethylene glycol) diblock copolymers by static and dynamic contact angle measurements, FTIR, and ATR-FTIR. *Langmuir*, *24*, 749–757.

Mishra, S., & Shimpi, N. G. (2007). Effect of the variation in the weight percentage of the loading and the reduction in the nanosizes of $CaSO_4$ on the mechanical and thermal properties of styrene-butadiene rubber. *Journal of Applied Polymer Science*, *104*, 2018–2026.

Mohanty, A. K., Misra, M., & Drzal, L. T. (2002). Sustainable bio-composites from renewable resources: Opportunities and challenges in the green materials world. *Journal of Polymers and the Environment*, *10*, 19–26.

Molnár, K., Móczó, J., Murariu, M., Dubois, P., & Pukánszky, B. (2009). Factors affecting the properties of PLA/$CaSO_4$ composites: Homogeneity and interactions. *Express Polymer Letters*, *3*, 49–61.

Mukhopadhyay, P., & Schreiber, H. P. (1995). Aspects of acid–base interactions and use of inverse gas-chromatography. *Colloids and Surfaces A-Physicochemical and Engineering Aspects*, *100*, 47–71.

Murariu, M., Ferreira, A. D., Degee, P., Alexandre, M., & Dubois, P. (2007). Polylactide compositions. Part 1: Effect of filler content and size on mechanical properties of PLA/calcium sulfate composites. *Polymer*, *48*, 2613–2618.

Murariu, M., Ferreira, A. D., Pluta, M., Bonnaud, L., Alexandre, M., & Dubois, P. (2008). Polylactide (PLA)–$CaSO_4$ composites toughened with low molecular weight and polymeric ester-like plasticizers and related performances. *European Polymer Journal*, *44*, 3842–3852.

Nagahama, K., Nishimura, Y., Ohya, Y., & Ouchi, T. (2007). Impacts of stereoregularity and stereocomplex formation on physicochemical, protein adsorption and cell adhesion behaviors of star-shaped 8-arms poly(ethylene glycol)–poly(lactide) block copolymer films. *Polymer*, *48*, 2649–2658.

Nielsen, L. E. (1974). *Mechanical properties of polymers and composites*. Marcel Dekker: New York.
Panzer, U., & Schreiber, H. P. (1992). On the evaluation of surface interactions by inverse gas-chromatography. *Macromolecules*, *25*, 3633–3637.
Parrinello, L. M. (1991). Fiber geometry-effects on physical-properties of chopped fiber composites. *Tappi Journal*, *74*, 85–88.
Paul, M. A., Alexandre, M., Degee, P., Henrist, C., Rulmont, A., & Dubois, P. (2003). New nanocomposite materials based on plasticized poly(L-lactide) and organo-modified montmorillonites: Thermal and morphological study. *Polymer*, *44*, 443–450.
Pluta, M., Jeszka, J. K., & Boiteux, G. (2007). Polylactide/montmorillonite nanocomposites: Structure, dielectric, viscoelastic and thermal properties. *European Polymer Journal*, *43*, 2819–2835.
Pluta, M., Murariu, M., Ferreira, A. D., Alexandre, M., Galeski, A., & Dubois, P. (2007). Polylactide compositions. II. Correlation between morphology and main properties of PLA/calcium sulfate composites. *Journal of Polymer Science Part B-Polymer Physics*, *45*, 2770–2780.
Pukánszky, B. (1992). Effect of interfacial interactions on the deformation and failure properties of PP/$CaCO_3$ composites. *New Polymeric Materials*, *3*, 205–217.
Pukánszky, B., & Vörös, G. (1996). Stress distribution around inclusions, interaction, and mechanical properties of particulate-filled composites. *Polymer Composites*, *17*, 384–392.
Razi, P. S., & Raman, A. (2000). Studies on impact fracture properties of wood–polymer composites. *Journal of Composite Materials*, *34*, 980–997.
Renner, K., Móczó, J., Vörös, G., & Pukánszky, B. (2010). Quantitative determination of interfacial adhesion in composites with strong bonding. *European Polymer Journal*, *46*, 2000–2004.
Renner, K., Yang, M. S., Móczó, J., Choi, H. J., & Pukánszky, B. (2005). Analysis of the debonding process in polypropylene model composites. *European Polymer Journal*, *41*, 2520–2529.
Rohman, G., Laupretre, F., Boileau, S., Guerin, P., & Grande, D. (2007). Poly(D,L-lactide)/poly(methyl methacrylate) interpenetrating polymer networks: Synthesis, characterization, and use as precursors to porous polymeric materials. *Polymer*, *48*, 7017–7028.
Sharpe, R., & Cork, G. (2006). In J. E. Kogel, N. C. Trivedi, J. M. Barker, & S. T. Krukowski (Eds.), *Gypsum and anhydrite. In Industrial minerals & rocks* (pp. 519–540). Littletown: Society for Mining, Metallurgy, and Exploration, Inc.
Sobkowicz, M. J., Feaver, J. L., & Dorgan, J. R. (2008). Clean and green bioplastic composites: Comparison of calcium sulfate and carbon nanospheres in polylactide composites. *Clean-Soil Air Water*, *36*, 706–713.
Södergard, A., & Stolt, M. (2002). Properties of lactic acid based polymers and their correlation with composition. *Progress in Polymer Science*, *27*, 1123–1163.
Wang, K., Wu, J., Ye, L., & Zeng, H. (2003). Mechanical properties and toughening mechanisms of polypropylene/barium sulfate composites. *Composites Part A: Applied Science and Manufacturing*, *34*, 1199–1205.
Wang, N., Zhang, X. X., Ma, X. F., & Fang, J. M. (2008). Influence of carbon black on the properties of plasticized poly(lactic acid) composites. *Polymer Degradation and Stability*, *93*, 1044–1052.
Williams, C. K., & Hillmyer, M. A. (2008). Polymers from renewable resources: A perspective for a special issue of polymer reviews. *Polymer Reviews*, *48*, 1–10.
Wypych, G. (1999). *Handbook of fillers*. Toronto: ChemTec Publishing.
Zebarjad, S. M., Tahani, M., & Sajjadi, S. A. (2004). Influence of filler particles on deformation and fracture mechanism of isotactic polypropylene. *Journal of Materials Processing Technology*, *155*, 1459–1464.
Zuiderduin, W. C. J., Westzaan, C., Huétink, J., & Gaymans, R. J. (2003). Toughening of polypropylene with calcium carbonate particles. *Polymer*, *44*, 261–275.